Available online at www.sciencedirect.com
SCIENCE DIRECT®
Surface Science 583 (2005) 36–45
SURFACE SCIENCE
www.elsevier.com/locate/susc

Analysis of the kinetics of N_2O–CO reaction on Pd(1 1 0)

Vladimir P. Zhdanov [a,b,*], Yunsheng Ma [a], Tatsuo Matsushima [a]

[a] *Catalysis Research Center, Hokkaido University, Sapporo 001-0021, Japan*
[b] *Boreskov Institute of Catalysis, Russian Academy of Sciences, Novosibirsk 630090, Russia*

Received 17 December 2004; accepted for publication 14 March 2005
Available online 31 March 2005

Abstract

Experimental studies indicate that the N_2O–CO reaction occurring on Pd(1 1 0) under UHV conditions exhibits a first-order kinetic phase transition in the steady-state case and also transient kinetics strongly dependent on the initial state of the system. We construct a mean-field kinetic model describing these phenomena. With a minimal number of the fitting parameters, the model reasonably reproduces the special features of the reaction kinetics.

Keywords: Computer simulations; Reaction kinetics; Kinetic phase transitions; Low index single crystal surfaces; Pd(1 1 0); N_2O; CO; N_2; Oxygen

1. Introduction

During or after adsorption of N_2O on Pt-group metals, one can observe N_2O decomposition accompanied by formation of adsorbed oxygen and N_2 desorption. The decomposition process is rather rapid. Under temperature-programmed conditions, it typically occurs below 200 K [1–5]. To run N_2O decomposition under steady-state conditions, one can remove adsorbed oxygen by CO. CO oxidation on Pt-group metals is well known to be also rapid. In particular, the steady-state kinetics of the CO–O_2 reaction is often controlled by reactant adsorption and/or blocking of adsorption sites by CO and accordingly exhibits a first-order kinetic phase transition (see, e.g., the review by Razon and Schmitz [6] and more recent experimental data for Pt(1 1 1) [7], Pt(1 1 0) [8], Ir(1 1 1) [9], and supported Pd [10]; for general theory of kinetic phase transitions, see Refs. [11,12]). In analogy with CO oxidation, this phenomenon is possible in the N_2O–CO reaction as well. In particular, it was observed by Sadnankar et al. [14] on alumina-supported Pt at atmospheric pressure. Recent experimental studies performed in our group [15] indicate that the N_2O–CO reaction exhibits a

* Corresponding author. Tel.: +7 3832 329513; fax: +7 3832 344687.
E-mail address: zhdanov@catalysis.nsk.su (V.P. Zhdanov).

0039-6028/$ - see front matter © 2005 Elsevier B.V. All rights reserved.
doi:10.1016/j.susc.2005.03.020

first-order kinetic phase transition also on Pd(1 1 0) under UHV conditions in the steady-state case. In addition, the transient kinetics are found to be strongly dependent on the initial state of the system. In this paper, we present a mean-field kinetic model of these phenomena. The results obtained are of interest from the point of view of theory of the kinetics of rapid catalytic reactions and also from the view-point of applied environmental chemistry [13], because N_2O is one of the harmful ingredients of motor vehicle gas.

The paper is organized as follows. First, we outline the key experimentally observed features of the reaction kinetics under consideration (Section 2). Our kinetic model is described in Section 3. The model parameters are validated in Section 4. The results of the calculations are shown and discussed in Section 5. Section 6 contains a brief summary.

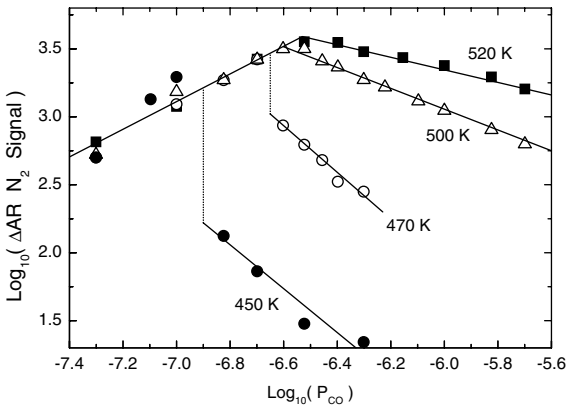

Fig. 1. N_2-desorption signal (arb. un.) as a function of CO pressure, P_{CO} (Torr), during N_2O–CO reaction on Pd(1 1 0) under steady-state conditions for $P_{N_2O} = 3.3 \times 10^{-6}$ Torr and surface temperatures of 450, 470, 500 and 520 K. The N_2-desorption rate was measured at 43° off normal into the [0 0 1] direction (at this angle, the rate is maximum). ΔAR means "angular resolved" (Δ indicates that the background N_2 signal has been subtracted).

2. Experimental data

The kinetics of the N_2O–CO reaction was studied on Pd(1 1 0) under UHV conditions by using the technique [1–5] allowing measurement of the angular-resolved distribution of desorbing species. The results focused on the temperature dependence of the reaction rate have already been published in a brief report [16]. More complete data including the pressure dependence of the reaction rate will be presented in detail elsewhere [15]. Here, we show typical steady-state and transient kinetics which are essential for our analysis and discussions below.

The specifics of the reaction under consideration is that the yield is small and accordingly we can hardly get an accurate angular-integrated signal. Fortunately, the angular-resolved signal is enhanced at around the collimation angle (43° off normal into the [0 0 1] direction) because of the sharp distribution, and can be used to follow the reaction. In particular, Fig. 1 exhibits the N_2-desorption rate measured under steady-state conditions at fixed N_2O pressure as a function of CO pressure at surface temperatures of 450, 470, 500 and 520 K. At $T_s \geqslant 500$ K, with increasing CO pressure, the rate of N_2 desorption first monotonously increases (in this region, the reaction rate is proportional to CO pressure), then reaches a maximum, and afterwards monotonously decreases. At lower temperatures, the N_2-desorption rate exhibits a stepwise behaviour classified as a first-order kinetic phase transitions. Such kinetic phase transitions are often associated with a hysteresis if pressure is changed back and forth (see e.g. experiments [7,9,10] and theory [11,12]). The width of a hysteresis may however be narrow or it can even be reduced to a single line corresponding to the equistability criterion [12]. The latter seems to happen in the reaction under consideration, because a hysteresis has not been observed in this case.

Fig. 2 shows the transient kinetics in the situation when first the reaction is run at steady state and then, at $t = 0$, the CO pressure is switched off. If under steady-state conditions the CO pressure is lower than that corresponding to the reaction-rate maximum (Fig. 2(a)), the N_2- and CO_2-desorption rates drop at $t > 0$ relatively slowly and almost instantaneously, respectively. If initially the CO pressure is higher than that associated with the reaction-rate maximum (Fig. 2(b)), the transient kinetics observed at $t > 0$ are somewhat more complex. Specifically, the N_2- and CO_2-desorption rates first increase and than after

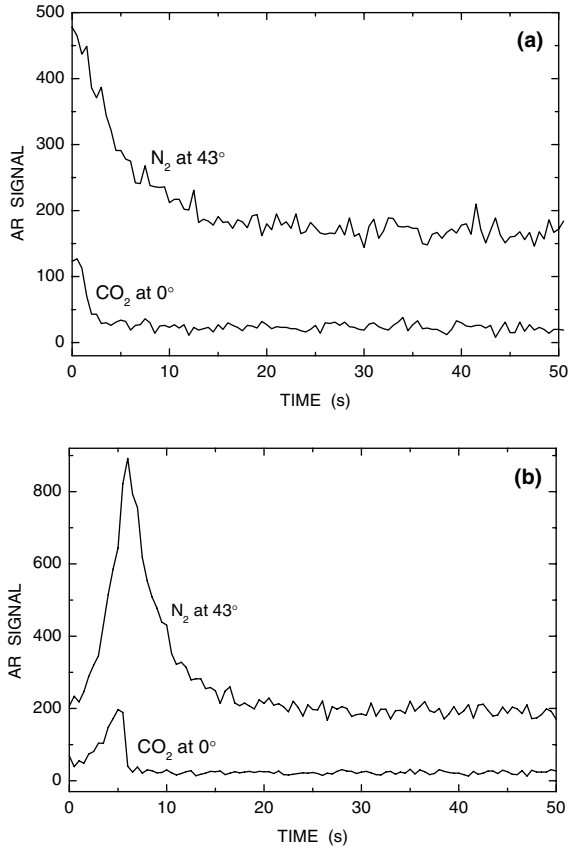

Fig. 2. N_2- and CO_2-desorption signals (arb. un.) measured as a function of time at respectively 43° and 0° off normal into the [0 0 1] direction (at these angles, the rates are maximum) in the situation when, after reaching a steady state at $T_s = 470$ K, $P_{N_2O} = 3.3 \times 10^{-6}$ Torr, and $P_{CO} = 0.1 \times 10^{-6}$ (a) and 0.5×10^{-6} Torr (b), the CO pressure was switched off (at $t = 0$). The background N_2 and CO_2 signals have not been subtracted. The time scale corresponding to the drop of the CO_2 signal in case (a) characterizes the switching-off procedure. Variation of the other signals is related to the reaction kinetics.

reaching a maximum decrease, respectively, relatively slowly and almost instantaneously.

3. Kinetic model

N_2O–CO reaction running on Pd(1 1 0) includes reversible adsorption on N_2O,

$$(N_2O)_{gas} \rightleftharpoons (N_2O)_{ad}. \quad (1)$$

Dissociation of adsorbed N_2O molecules results in the formation of adsorbed oxygen and N_2 desorption. Under TPD conditions [2], N_2 desorption dominates compared to N_2O desorption. Specifically, the N_2 TPD spectra exhibit four peaks, β_1–β_4, located at temperatures between 90 and 170 K, or more specifically at $\simeq$110 (β_4), 125 (β_3), 138 (β_2), and 150 K (β_1). The angular distribution of the flux of desorbing N_2 molecules is close to cosine for the β_2 peak while in other cases the flux is collimated either at $\simeq$43° (for the β_1 and and β_3 peaks) or at 50° (for the β_4 peak) off normal into the [0 0 1] direction. The cosine distribution is suggestive of desorption of adsorbed N_2 molecules formed after N_2O dissociation,

$$(N_2O)_{ad} \rightarrow (N_2)_{ad} + O_{ad}, \quad (2)$$

$$(N_2)_{ad} \rightarrow (N_2)_{gas}. \quad (3)$$

The inclined flux is related to N_2 molecules desorbing during N_2O dissociation,

$$(N_2O)_{ad} \rightarrow (N_2)_{gas} + O_{ads}. \quad (4)$$

In the latter case, the splitting of the N_2 TPD signal seems to be primarily due to the N_2O–O lateral interactions (see e.g. interpretation [17] of similar TPD spectra observed during N_2O decomposition on Rh(1 1 0)).

In principle, the gas-phase N_2O may react with adsorbed oxygen [18],

$$(N_2O)_{gas} + O_{ad} \rightarrow (N_2)_{gas} + (O_2)_{gas},$$

but on Pd(1 1 0) this step does not seem to occur.

In addition to steps (1)–(4), we have reversible CO adsorption,

$$(CO)_{gas} \rightleftharpoons (CO)_{ad}, \quad (5)$$

and the Langmuir–Hinshelwood (LH) reaction between adsorbed CO and oxygen,

$$(CO)_{ad} + O_{ad} \rightarrow (CO_2)_{gas}. \quad (6)$$

In applied environmental chemistry, the N_2O–CO reaction is usually considered to be a subreaction of the NO–CO reaction [13]. Specifically, the N_2O formation is believed to occur as

$$(NO)_{ad} + N_{ad} \rightarrow (N_2O)_{ads},$$

or

$$(NO)_{ad} + (NO)_{ad} \rightarrow (N_2O)_{ads} + O_{ads}.$$

For our present discussion, these steps are however irrelevant.

Thus, the reaction scheme we use includes steps (1)–(6). Basically, this scheme is close to those proposed by Sadnankar et al. [14] and McCabe and Wong [19] for interpretation of the steady-state kinetics of the N_2O–CO reaction on alumina-supported Pt and Rh, respectively.

To simplify the treatment of the reaction kinetics, we take into account that N_2O dissociation and desorption and N_2 desorption are rapid. Under TPD conditions, as already mentioned, these steps occur at temperatures between 90 and 170 K. This means that the corresponding activation energies are in the range from 5 to 12 kcal/mol (for the DFT calculations of the N_2O binding energies on Pd(1 1 0), see Ref. [20]) and accordingly under steady-state or transient conditions at relatively high temperatures (e.g., between 450 and 520 K as in the cases shown in Figs. 1 and 2) the N_2O and N_2 coverages are very low. For these reasons, we may always use the steady-state approximation in order to describe N_2O dissociation and desorption and N_2 desorption. More specifically, we replace steps (1)–(3) by a N_2O adsorption step accompanied by dissociation resulting in instantaneous N_2 desorption (for details, see Section 4.1 below). The surface is considered to be covered only by CO or O. The equations for coverages of these species are as follows

$$d\theta_O/dt = k^{ad}_{N_2O} P_{N_2O} - k_{LH}\theta_O\theta_{CO}, \quad (7)$$

$$d\theta_{CO}/dt = k^{ad}_{CO} P_{CO} - k^{des}_{CO}\theta_{CO} - k_{LH}\theta_O\theta_{CO}, \quad (8)$$

where P_{N_2O} and P_{CO} are the reactant pressures, $k^{ad}_{N_2O}$ is the rate constant of N_2O adsorption accompanied by dissociation resulting in N_2 desorption, k^{ad}_{CO} and k^{des}_{CO} are the rate constants for CO adsorption and desorption, k_{LH} is the rate constant of the LH step. The coverage dependence of these rate constants is discussed in the next section.

4. Specification of the reaction steps

The kinetics of rapid catalytic reactions are sensitive to the coverage dependence of the rates of reactant adsorption and desorption [12]. Below, we discuss these steps in detail. In particular, we take into account the effect of oxygen-induced surface restructuring on the rate of N_2O adsorption. The LH step is discussed briefly. The influence of surface restructuring on the latter step is neglected, because the step is rapid anyway and its specific does not matter. In addition, the reaction kinetics can under certain conditions be complicated by surface-oxide formation. In our present model, the latter process is neglected, because at present its role is open for debate.

4.1. N_2O adsorption and dissociation

After adsorption, N_2O molecules may dissociate via channels (2) and (4). The activation energy for channel (2) is slightly lower than that for channel (4), because at low temperatures under TPD conditions the intensity of the corresponding N_2 TPD peak (β_2, with a cosine angular distribution) is comparable or higher than those of the other N_2 peaks [2]. At temperatures about 500 K, the N_2 flux is however collimated at $\simeq 43°$ [16,15] like in the case of the β_1 and β_3 N_2 TPD peaks. This indicates that at these temperatures channel (4) is more important due to the entropic factor or, more specifically, due to a higher value of the pre-exponential factor of the corresponding rate constant (according to the transition state theory, the pre-exponential factor is proportional to the partition function of an activated complex, and this function is expected to be larger for channel (4)). In our treatment, N_2O dissociation is accordingly assumed to occur via channel (4).

At temperatures about 500 K, the LH step is rapid and accordingly during the N_2O–CO reaction in analogy with the CO–O_2 reaction the Pd surface is primarily covered either by O or CO. Under steady-state conditions, these two regimes take place respectively to the left and right from the reaction-rate maximum (Fig. 2(a)). The distributions of O and CO on the Pd(1 1 0) surface are different and accordingly the corresponding coverage dependences of $k^{ad}_{N_2O}$ are expected to be different as well.

In particular, oxygen adsorption typically results in surface restructuring with the formation of anisotropic (1×2) "missing-row" islands

[21,22]. The corresponding LEED patterns are of the $c(2\times4)$ symmetry. During CO oxidation by oxygen and N_2O, the LEED patterns are also indicative of the formation of the (1×2) or (1×3) "missing-row" islands (see Refs. [23,15], respectively) provided that the CO pressure is sufficiently low (to the left from the reaction-rate maximum in Fig. 1). This means that oxygen and Pd diffusion is rapid compared to the LH step and oxygen is able to migrate and to induce the island formation. To be specific, we assume in our calculations that the islands are of the (1×2) type. In this case, the local oxygen coverage inside such islands is 0.5 and accordingly the fraction of the surface covered by islands is $2\theta_O$. (For the (1×3) islands, the corresponding fraction, $3\theta_O$, is somewhat higher. This difference is however insignificant for our presentation below.)

N_2O molecules may adsorb both inside and outside the "missing-row" islands. Inside the islands, N_2O dissociation seems to be suppressed due to spatial constraints. Diffusion of N_2O molecules from these islands to the (1×1) area is expected to be suppressed as well due to rapid desorption (the activation energy for N_2O desorption is somewhat higher than for diffusion, but this can be compensated by a higher pre-exponential factor [24]). For these reasons, N_2O decomposition seems to occur primarily due to adsorption and dissociation on the (1×1) patches. This explains why during the reactive conditions with surface restructuring the N_2 angular distribution is collimated at $\simeq43°$ like in the TPD case on the (1×1) surface.

Thus, in the situation when the surface is primarily covered by oxygen, the rate constant of N_2O adsorption accompanied by dissociation and N_2 desorption can be represented as

$$k^{ad}_{N_2O} = (1-2\theta_O)p_{dis}\kappa^{ad}_{N_2O}, \tag{9}$$

where $(1-2\theta_O)$ is the fraction of the surface remaining in the (1×1) state, $\kappa^{ad}_{N_2O}$ is the N_2O impingement rate constant, and p_{dis} is the dissociation probability given by

$$p_{dis} = \kappa_{dis}/(\kappa_{dis}+\kappa_{des}), \tag{10}$$

where κ_{dis} and κ_{des} are the N_2O dissociation and desorption rate constants.

Eq. (9) predicts that the rate of N_2O adsorption accompanied by dissociation linearly decreases with increasing oxygen coverage and that the saturation of the overlayer takes place at $\theta_O = 0.5$. Both these predictions are in good agreement with measurements [25] of the apparent sticking coefficient for N_2O adsorption and dissociation at $T_s \simeq 500$ K (at much lower temperatures, the oxygen diffusion is slow and the saturation oxygen coverage may be higher than 0.5 ML). At these temperatures, the dissociation probability p_{dis} is appreciably lower than unity [25]. This means that $\kappa_{dis} \ll \kappa_{des}$ and accordingly Eq. (10) can be rewritten as

$$p_{dis} = \kappa_{dis}/\kappa_{des}, \tag{11}$$

or

$$p_{dis} = p_0 \exp(\Delta E/k_B T), \tag{12}$$

where p_0 and ΔE are respectively the ratio of the pre-exponential factors and the difference of the activation energies for dissociation and desorption.

Adsorbed CO may also induce "missing-row" restructuring of the Pd(1 1 0) surface [28]. Under reactive conditions at $T_s \simeq 500$ K, it does not seem to occur, because the surface exhibits the (1×1) LEED pattern [15,23]. Practically, this means that dissociation of N_2O molecules occurs among CO molecules, and accordingly in analogy with NO dissociation e.g. on Rh(1 1 1) [26] the N_2O dissociation rate may rapidly drop with increasing CO coverage due to N_2O–CO lateral interactions. For this reason, in the situation when the surface is primarily covered by CO, the rate constant $k^{ad}_{N_2O}$ can be represented as [27]

$$k^{ad}_{N_2O} = (1-\theta_{CO})^n p_{dis}\kappa^{ad}_{N_2O}, \tag{13}$$

where p_{dis} is the dissociation probability at low coverages (Eq. (12)), and $n \geqslant 2$ is the exponent used below as a fitting parameter (the fact that n may be above 2 means that due to lateral interactions the dissociation becomes more probable when a N_2O molecule has more nearest-neighbour vacant sites but it does not necessarily mean that the dissociation is possible only if a molecule has several vacant sites [27]).

Expressions (9) and (13) for $k^{ad}_{N_2O}$ are applicable when the surface is covered either by O or CO. In calculations, it is convenient to use a single expression for $k^{ad}_{N_2O}$, given by combination of Eqs. (9) and (13),

$$k^{ad}_{N_2O} = (1 - 2\theta_O)(1 - \theta_{CO})^n p_{dis} \kappa^{ad}_{N_2O}. \quad (14)$$

4.2. CO adsorption and desorption

CO adsorption on Pt-group metals usually occurs via precursor states and the effect of oxygen on the adsorption rate is weak. Neglecting this effect, we use the following simplest expression for the rate constant of precursor-mediated CO adsorption

$$k^{ad}_{CO} = [(1 - \theta_{CO})/(1 - \theta_{CO} + p\theta_{CO})]\kappa^{ad}_{CO}, \quad (15)$$

where κ^{ad}_{CO} is the CO impingement rate constant, and $p < 1$ is the parameter related to the precursor states. In agreement with experiment [28], Eq. (15) implies that the CO sticking coefficient is close to unity at low coverages.

The CO-desorption rate constant is represented as

$$k^{des}_{CO} = \nu_{des} \exp[-(E_{des} - A\theta_{CO})/k_B T], \quad (16)$$

where ν_{des} is the pre-exponential factor, E_{des} is the activation energy at low coverages, and $A > 0$ is the parameter related to repulsive lateral CO–CO interactions.

4.3. Reaction between adsorbed CO and O

The rate constant for the LH reaction between adsorbed CO and O usually depend on adsorbate-adsorbate lateral interactions. The effect of this dependence on the reaction kinetics is however minor, because anyway the LH step is fast compared to N_2O and CO adsorption and CO desorption. For this reason, we employ the simplest expression for the LH-reaction rate constant,

$$k_{LH} = \nu_{LH} \exp(-E_{LH}/k_B T), \quad (17)$$

where ν_{LH} and E_{LH} are the coverage-independent Arrhenius parameters.

Table 1
Kinetic parameters used in the calculations

Parameter	Value	Dimension	Ref.
$k^{ad}_{N_2O}$			Eq. (14)
p_0	2×10^{-3}	–	AM [25]
ΔE	4	kcal/mol	AM [25]
n	4	–	Fitting
$\kappa^{ad}_{N_2O}$	3.38×10^5	$s^{-1}Torr^{-1}$	KT
k^{ad}_{CO}			Eq. (15)
p	0.3	–	AM [28]
κ^{ad}_{CO}	4.09×10^5	$s^{-1}Torr^{-1}$	KT
k^{des}_{CO}			Eq. (16)
ν_{des}	10^{16}	s^{-1}	TST [24]
E_{des}	38	kcal/mol	TPD [28]
A	7	kcal/mol	TPD [28]
k_{LH}			Eq. (17)
ν_{LH}	10^{12}	s^{-1}	TST [24]
E_{LH}	22	kcal/mol	DFT [29]

All the values (except n) were obtained either from general theory or on the basis of independent experimental data presented in the corresponding references.

4.4. Kinetic parameters

The values of the kinetic parameters used in Eqs. (12) and (14)–(17) were obtained (Table 1) by employing the results of independent adsorption measurements (AM), TPD experiments, elementary kinetic theory (KT), transition-state theory (TST), and results of calculations based on the density-functional theory (DFT). The only fitting parameter is the exponent n in Eq. (14).

5. Results of calculations

Our model is based on Eqs. (7) and (8) combined with expressions (14)–(17) for the rate constants for the elementary reaction steps. To use the model, we should specify the exponent n in the rate constant (14) describing N_2O adsorption and dissociation. If the probabilities of adsorption and dissociation on the surface covered by CO were proportional to $(1 - \theta_{CO})$, one would have $n = 2$. With this exponent, the model predicts a kinetic phase transition but its shift to lower CO pressures with decreasing temperature is much weaker compared to that observed in the

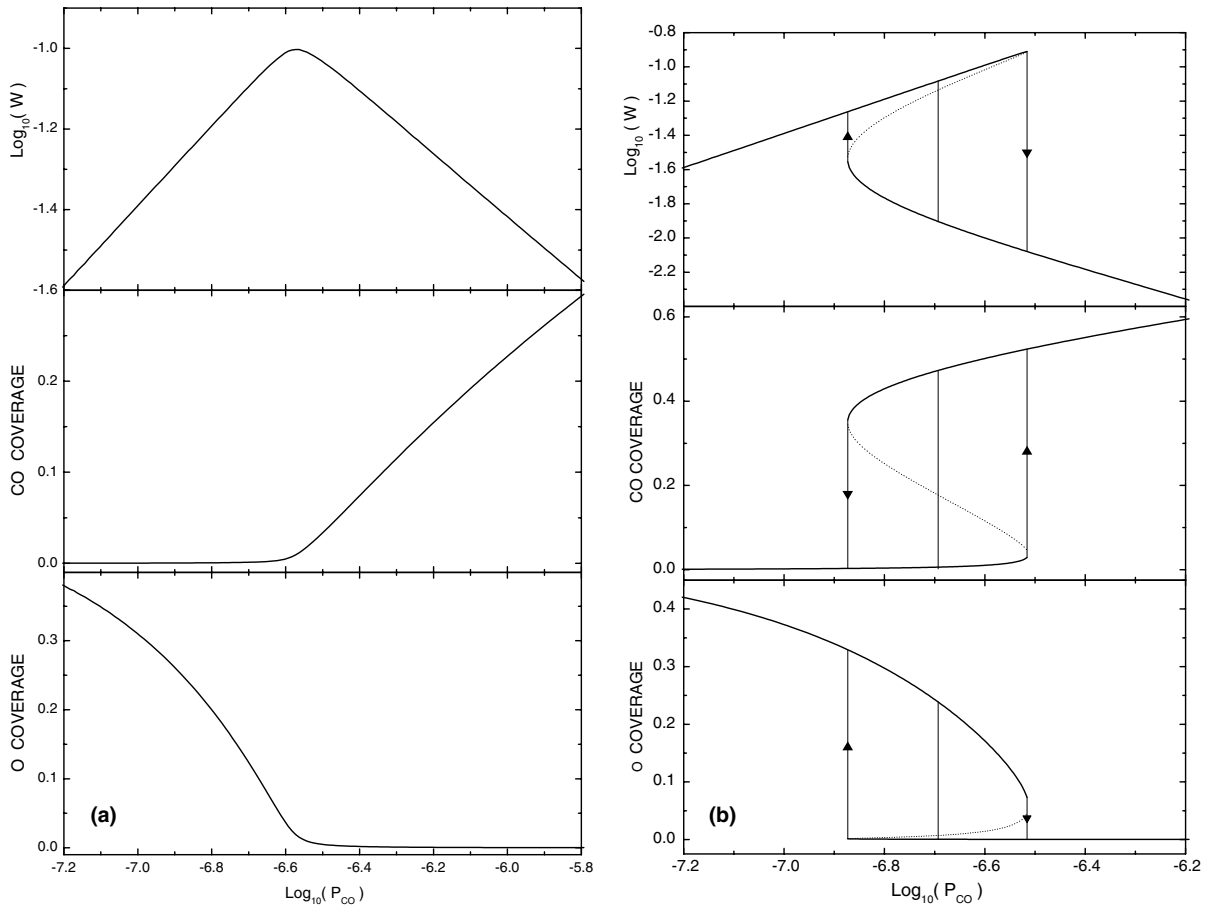

Fig. 3. Rate of N_2 or CO_2 formation, W (ML/s), and CO and O coverages as a function of CO pressure, P_{CO} (Torr), calculated under steady-state conditions for $P_{N_2O} = 3.3 \times 10^6$ Torr and $T_s = 520$ (a) and 470 K (b). In the latter case, the model predicts a first-order kinetic phase transition or, more specifically, bistablity. The stable and unstable solutions are indicated by the thick and dashed lines, respectively. The thin solid lines marked by arrows show hysteresis. The thin solid line located between the latter lines corresponds to the equistability condition (the exact location of this line slightly depends on the details of the interplay between reaction kinetics and diffusion of adsorbed species [12]).

experiment (Fig. 1). To reproduce the experimentally observed shift, we use $n = 4$. The fact that $n > 2$ physically means that the N_2O dissociation rate rapidly decreases with increasing CO coverage due to N_2O–CO lateral interactions in the activated state for N_2O dissociation [27].

Typical steady-state reaction kinetics calculated above and below the critical temperature are shown in Fig. 3(a) and (b), respectively. If CO pressure is lower than that corresponding to the reaction-rate maximum, the model is seen to predict in analogy with CO oxidation and in agreement with the experiment that the reaction rate is proportional to CO pressure, because in this case it is determined by the rate of CO adsorption on the surface covered primarily by oxygen (CO desorption here is nearly negligible). For higher CO pressures, also in analogy with CO oxidation, the surface is mainly covered by CO, CO is typically close to the adsorption–desorption equilibrium, and accordingly the reaction rate drops with increasing CO pressure, because it is deter-

mined by N_2O adsorption and dissociation on the CO-covered surface.

Below the critical temperature, the model or more specifically Eqs. (7) and (8) predict a well-developed hysteresis as shown in Fig. 3(b). Note that the corresponding stable and unstable solutions, indicated respectively by the thick and dashed lines, are stable and unstable with respect to *temporal* perturbations. *Spatio-temporal* perturbations and/or fluctuations may reduce the width of the hysteresis or, as already mentioned in Section 2, may result in the stepwise transition along the equistability line with no hysteresis. Whether it happens in reality depends on the details of nucleation and propagation of kinetic phases or, in other words, of chemical waves [12].

The equistability condition corresponds to the case when the rate of a chemical wave describing the interplay of two kinetic phase (one is e.g. on one side of the surface and another one on the other side) is equal zero. Usually, the equistability line is located near the middle of the bistability window. To get the equistability condition, one should analyze the propagation of a chemical wave, i.e., to solve the diffusion-reaction equations. For the conventional models of CO oxidation, this can be easily done (see, e.g., Ref. [12]) and one can obtain explicit expression for the equistability condition. In our case, the propagation of chemical waves depends not only on reaction steps and adsorbate diffusion, but also on the details of adsorbate-induced surface restructuring, and the corresponding analysis is far from trivial.

From the theoretical point of view, the situation with the formation of critical nuclei is far from trivial as well not only for the NO_2–CO reaction but also for CO oxidation. For the latter reaction on Pt(1 1 1) [7], Pt(1 1 0) [8], Ir(1 1 1) [9], and supported Pd [10], one can observe hysteresis. In our case, the measured reaction kinetics does not however show hysteresis. One of the probable reasons of this finding is that the nucleation of kinetic phases on Pd(1 1 0) might be related to oxygen-induced surface restructuring and accordingly it might be facilitated due to thermodynamic driving forces.

Assuming the kinetic phase transition to occur at the equistability point and that this point to be located at the middle of the bistability window, we have constructed Fig. 4, which can be directly compared with the experimental data shown in Fig. 1. The agreement between the experiment and calculations is seen to be good.

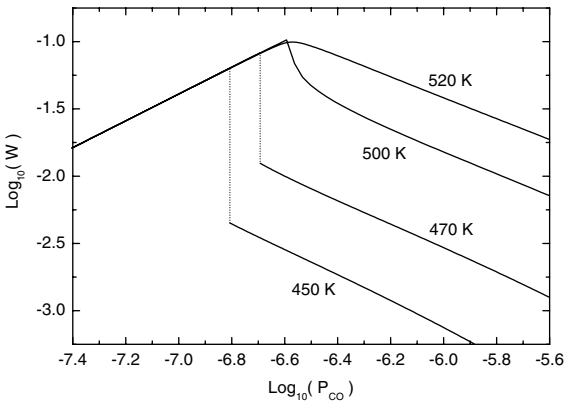

Fig. 4. Rate of N_2 or CO_2 formation, W (ML/s), and CO and O coverages as a function of CO pressure, P_{CO} (Torr), calculated under steady-state conditions for $P_{N_2O} = 3.3 \times 10^{6}$ Torr and $T_s = 450$, 470, 500, and 520 K. The dashed lines indicating a first-order kinetic phase transition correspond to the equistability condition.

The transient reaction kinetics predicted by the model are in good agreement with the experiment as well (cf. Figs. 2 and 5). In particular, the model reasonably reproduces all the special features of the reaction kinetics measured after switching off CO pressure.

Finally, it is appropriate to articulate that the reaction under consideration is rapid and accordingly the reaction rate (or more specifically the rate of N_2 desorption) can be identified with that of N_2O dissociative adsorption both under steady-state and transient conditions (this identification is exact in the former case and very accurate in the latter case). In our simulations, the value of the rate constant for the latter step was chosen by using the data reported in Ref. [25]. The measurements performed in our group are in agreement with those presented in Ref. [25]. Thus, we can conclude that our measurements (Figs. 1 and 2) and calculations (Figs. 4 and 5) are in reasonable quantitative agreement despite the fact that that the measured reaction rates are presented in arbitrary units.

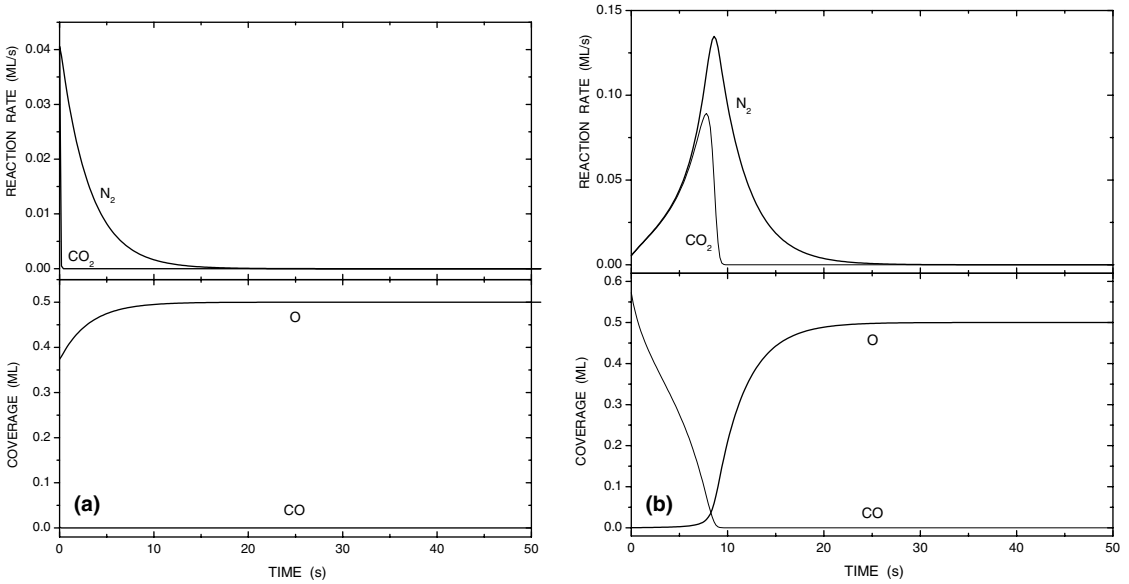

Fig. 5. Rate of N_2 or CO_2 formation and CO and O coverages as a function of time calculated for the situation (as in Fig. 2) when, after reaching a steady state at $T_s = 470$ K, $P_{N_2O} = 3.3 \times 10^{-6}$ Torr, and $P_{CO} = 0.1 \times 10^{-6}$ (a) and 0.5×10^{-6} Torr (b), the CO pressure is switched off (at $t = 0$).

6. Conclusion

We have constructed a mean-field kinetic model of the N_2O–CO reaction on Pd(110). With a minimum number of the fitting parameters, it reasonably describes the first-order kinetic phase transition, observed in this reaction under steady-state conditions, and also the transient kinetics. In addition, we have discussed why the steady-state kinetics do not exhibit hysteresis. The latter aspect of the problem remains however open for further theoretical analysis.

Acknowledgement

One of the authors (V.P. Zh.) is grateful for the Guest Professorship at the Catalysis Research Center, Hokkaido University.

References

[1] Y. Ohno, K. Kimura, M. Bi, T. Matsushima, J. Chem. Phys. 110 (1999) 8221.
[2] H. Horino, S.W. Liu, A. Hiratsuka, Y. Ohno, T. Matsushima, Chem. Phys. Lett. 341 (2001) 419.
[3] H. Horino, I. Rzeznicka, A. Kokalj, I. Kobal, A. Hiratsuka, Y. Ohno, T. Matsushima, J. Vac. Sci. Technol. A 20 (2002) 1592.
[4] K. Imamura, H. Horino, I. Rzenicka, I. Kobal, A. Kokalj, Y. Ohno, B.E. Nieuwenhuys, A. Hiratsuka, T. Matsushima, Surf. Sci. 566 (2004) 1076.
[5] T. Matsushima, Surf. Sci. Rep. 52 (2003) 1.
[6] L.F. Razon, R.A. Schmitz, Catal. Rev. Sci. Eng. 28 (1986) 89.
[7] M. Berdau, G.G. Yelenin, A. Karpowicz, M. Ehsasi, K. Christmann, J.H. Block, J. Chem. Phys. 110 (1999) 11551.
[8] B.L.M. Hendriksen, J.W.M. Frenken, Phys. Rev. Lett. 89 (2002) 046101.
[9] S. Wehner, F. Baumann, J. Kuppers, Chem. Phys. Lett. 370 (2003) 126.
[10] V. Johanek, M. Laurin, A.W. Grant, B. Kasemo, C.R. Henry, J. Libuda, Science 304 (2004) 1639.
[11] J.W. Evans, Langmuir 7 (1991) 2514.
[12] V.P. Zhdanov, B. Kasemo, Surf. Sci. Rep. 20 (1994) 111.
[13] V.P. Zhdanov, B. Kasemo, Surf. Sci. Rep. 29 (1997) 31.
[14] R.R. Sadnankar, J. Ye, D.T. Lynch, J. Catal. 146 (1994) 511.
[15] Y. Ma, T. Matsushima, Langmuir, submitted.
[16] Y. Ma, I. Kobal, T. Matsushima, J. Phys. Chem. 109 (2005) 689.
[17] V.P. Zhdanov, T. Matsushima, Surf. Sci., in press, doi:10.1016/j.susc.2005.03.043.

[18] R. Burch, S.T. Daniells, J.P. Breen, P. Hu, J. Catal. 224 (2004) 252.
[19] R.W. McCabe, C. Wong, J. Catal. 121 (1990) 422.
[20] A. Kokalj, I. Kobal, T. Matsushima, J. Phys. Chem. B 107 (2003) 2741.
[21] H. Tanaka, J. Yoshinobu, M. Kawai, Surf. Sci. 327 (1995) L505.
[22] R.A. Bennett, S. Poulston, I.Z. Jones, M. Bowker, Surf. Sci. 401 (1998) 72.
[23] I. Rezeznicka, T. Matsushima, Chem. Phys. Lett. 377 (2003) 279.
[24] V.P. Zhdanov, Elementary Physicochemical Processes on Solid Surfaces, Plenum, New York, 1991.
[25] S. Haq, A. Hodgson, Surf. Sci. 463 (2000) 1.
[26] H.J. Borg, J.F.C.-J.M. Reijerse, R.A. van Santen, J.W. Niemantsverdriet, J. Chem. Phys. 101 (1994) 10052.
[27] V.P. Zhdanov, B. Kasemo, J. Chem. Phys. 104 (1996) 2446.
[28] K. Yagi-Watanabe, H. Fukutani, J. Chem. Phys. 112 (2000) 7652.
[29] Z.P. Liu, P. Hu, Topics Catal. 28 (2004) 71.